Cyclic N-locked indolicidin analogues with antimicrobial activity

Effect of ring size and fatty acid acylation

Lone, Abdullah; Nielsen, Josefine Eilsø; Thulstrup, Peter W.; Lund, Reidar; Hansen, Paul Robert; Jenssen, Håvard

Published in:
European Journal of Medicinal Chemistry Reports

DOI:
10.1016/j.ejmcr.2022.100080

Publication date:
2022

Document Version
Publisher's PDF, also known as Version of record

Citation for published version (APA):
Lone, A., Nielsen, J. E., Thulstrup, P. W., Lund, R., Hansen, P. R., & Jenssen, H. (2022). Cyclic *N*-locked indolicidin analogues with antimicrobial activity: Effect of ring size and fatty acid acylation. *European Journal of Medicinal Chemistry Reports*, *6*, [100080]. https://doi.org/10.1016/j.ejmcr.2022.100080

European Journal of Medicinal Chemistry Reports 6 (2022) 100080

HOSTED BY

Contents lists available at ScienceDirect

European Journal of Medicinal Chemistry Reports

journal homepage: www.editorialmanager.com/ejmcr/default.aspx

Cyclic *N*-locked indolicidin analogues with antimicrobial activity: Effect of ring size and fatty acid acylation

Abdullah Lone [a,b], Josefine Eilsø Nielsen [c,1], Peter W. Thulstrup [d], Reidar Lund [c], Paul Robert Hansen [b], Håvard Jenssen [a,*]

[a] Department of Science and Environment, Roskilde University, Universitetsvej 1, 4000, Roskilde, Denmark
[b] Department of Drug Design and Pharmacology, Faculty of Health and Medical Sciences, University of Copenhagen, Universitetsparken 2, 2100, Copenhagen, Denmark
[c] Department of Chemistry, University of Oslo, Sem Sælands vei 26, 0371, Oslo, Norway
[d] Department of Chemistry, University of Copenhagen, Universitetsparken 5, 2100, Copenhagen, Denmark

ARTICLE INFO

Keywords:
Antimicrobial peptides
Cyclic antimicrobial peptides
Cyclic indolicidin
Cyclic lipopeptides
Circular dichroism
Small-angle X-ray scattering

ABSTRACT

Novel antimicrobial drugs are in high demand due to the increasing emergence of multi-drug resistant bacteria. In recent years, much attention has been given to natural occurring antimicrobial peptides (AMPs) such as indolicidin (ILPWKWPWWPWRR-NH_2). In this study, 19 cyclic *N*-locked indolicidin analogues (**3**–**21**) were synthesized successfully by standard 9-fluorenylmethoxycarbonyl (Fmoc) solid-phase peptide synthesis (SPPS) combined with a convenient on-resin *N*-terminus to lysine side-chain cyclization via intramolecular halide substitution using bromoacetic acid. The effect of the ring size on antimicrobial activity and cytotoxicity was initially investigated and subsequently, the effect of fatty acid acylation was explored. We observed that a peptide macrocycle consisting of seven residues was optimal for Gram-positive antibacterial activity. Circular dichroism (CD) spectra of peptide macrocycles (**3**–**13**) showed that certain positions of ring-closure induced a conformation seen under sodium dodecyl sulfate (SDS) conditions where Trp side-chains can display exciton coupling. The far-UV CD was consistent with a backbone turn, a conformation with no evidence of helical structure. SAXS data on peptides mixed with lipid vesicles indicate a similar membrane interaction, when comparing the cyclic and linear indolicidin. The most potent analogue identified was **7**, which showed antibacterial activity against Gram-positive bacteria (MIC against *Staphylococcus aureus* ATCC29213 = 12.5 μg/mL and *Staphylococcus epidermidis* HJ56 = 6.3 μg/mL). In addition, viable HaCaT cells after 200 μg/mL treatment with **7** was 84.3%. The results show that *N*-locked cyclization of linear antimicrobial peptides provides a method to reduce cytoxicity; although it may affect the antimicrobial activity.

1. Introduction

Modern medicine has flourished due to the introduction of antimicrobial drugs in the 1940s [1]. However, over-prescription and misuse of these have led to global health crisis where Multi-drug resistant bacteria are common [2]. The opportunistic ESKAPE pathogens in nosocomial infections such as *Enterococcus faecium*, *Staphylococcus aureus*, *Klebsiella pneumoniae*, *Acinetobacter baumannii*, *Pseudomonas aeruginosa* and *Enterobacter* spp are particularly problematic [3].

Novel antimicrobial drugs are in demand and much attention has been given to naturally occurring antimicrobial peptides (AMPs) [4]. AMPs are relatively short (6–40 amino acids), positively charged (net charge of +2 to +9) and amphipathic [5]. However, the clinical success of AMPs may have been limited by their susceptibility to proteases, low bioavailability and potential toxicity [6]. The stability of AMPs can be improved by insertion of non-proteinogenic building blocks [6], cyclization [7] or through modification of the peptide backbone [8,9]. Indolicidin is a natural cationic tridecapeptide amide (ILPWKWPWWPWRR-NH_2) isolated from the cytoplasmic granules of bovine neutrophils [10]. It possesses broad-spectrum antimicrobial activity against Gram-positive and Gram-negative bacteria [11]. However, indolicidin has been shown to be strongly cytotoxic [12] exhibiting an extended structure when bound to membranes [13]. Both membrane effects and intracellular targets have been proposed [14], but studies by

* Corresponding author.
E-mail address: jenssen@ruc.dk (H. Jenssen).
[1] Current address: Department of Bioengineering, Stanford University, Stanford, California, 94305, United States.

https://doi.org/10.1016/j.ejmcr.2022.100080
Received 27 June 2022; Accepted 28 August 2022
Available online 5 September 2022

Nielsen et al. showed that indolicidin is believed to work by the interfacial activity model, causing a disordering of the lipids in the bilayer by inserting in the interface between the lipid head and tail region [15,16]. Several modifications to the sequence have been reported from structure-activity studies [17], peptide-peptoid hybrids [18], to cyclic analogues by formation of a disulfide bridge between two cysteine residues [19]. To our knowledge, the indolicidin sequence has not been utilized for design of cyclic lipopeptide antimicrobials. The group of naturally occurring cyclic lipopeptide antibiotic includes polymyxin B, polymyxin E (colistin) [20] and daptomycin [21], which are considered to be last resort antibiotics. Therefore, we wanted to investigate alternative cyclic analogues of indolicidin with possible parallel characteristics as the polymyxins or daptomycin. In this study, 19 cyclic *N*-locked indolicidin analogues (3–21) were synthesized successfully by Fmoc solid phase peptide synthesis (SPPS) (See Scheme 1). The analogues were prepared by on-resin N-terminus to lysine side-chain cyclization via an intramolecular halide substitution [22]. This furnishes a secondary amine which allows further derivatization e.g. lipidation. The antimicrobial activity of the analogues was tested against four bacterial strains: *S. aureus* ATCC29213, *S. epidermidis* HJ56, *P. aeruginosa* H103 and *Escherichia coli* ATCC25922 and cytotoxicity were evaluated against the human keratinocyte cell line HaCaT. Finally, circular dichroism and SAXS were used to investigate the structural variations of 3–13 compared with indolicidin.

2. Materials and methods

2.1. Materials and instruments

For materials and instruments used for chemical synthesis,

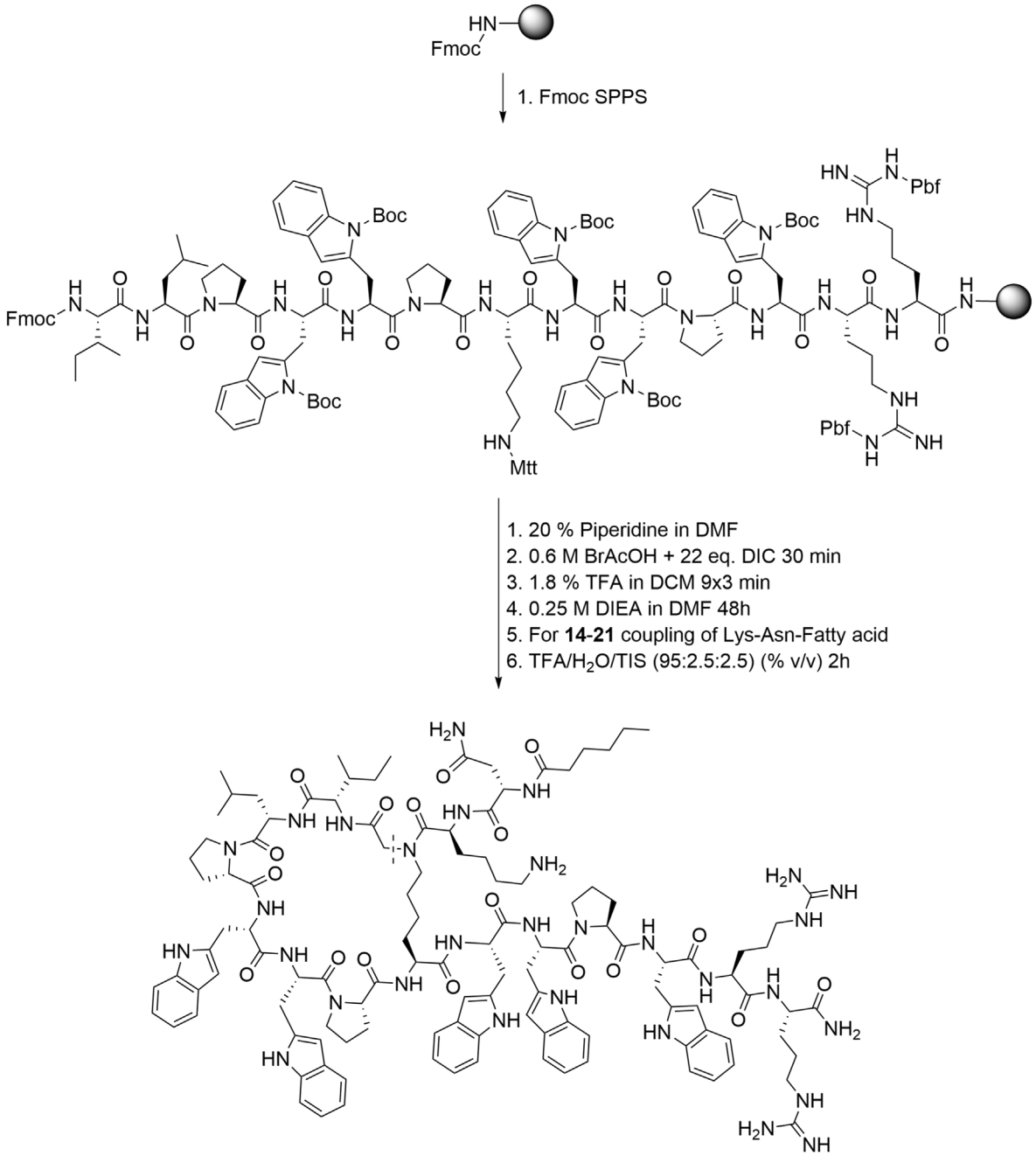

Scheme 1. Strategy for the synthesis of cyclic *N*-locked indolicidin analogues (synthesis of **14** is shown). The dashed line highlights the cyclization point.

purification, mass characterization, minimum inhibitory concentration and cytotoxicity experiment, see supplementary materials S1.

2.2. Peptide synthesis

The peptides were synthesized by standard Fmoc SPPS chemistry on a TentaGel S RAM resin (0.22 mmol/g) [23]. The TentaGel S RAM resin (200 mg) was weighed into disposable 5 mL syringes and was swelled overnight in DMF. The Fmoc group was removed using a 20% piperidine in DMF solution (*v/v*) 3 times of 4 min each (7 min each when >7 amino acids were coupled to the resin). An excess of 4 equivalents of amino acids, HATU and HOAt and 8 equivalents of DIEA relative to the resin loading were used for the couplings. Couplings were performed as single couplings with a coupling time of 2 h at room temperature. The washes consisted of a quick wash (wash 3 times with DMF) performed in between the Fmoc removal steps and a full wash (wash 3 times with DMF, 3 times with DCM and 5 times with DMF) performed after the final Fmoc removal step and after completed coupling.

2.3. Bromoacetic acid acylation

The acylation step on the N-terminus was accomplished using 20 equivalents of bromoacetic acid (BrAcOH) in DMF (0.6 M) and 22 equivalents of DIC for 30 min.

2.4. Removal of Mtt group

After coupling of bromoacetic acid to the N-terminus, the resin was washed 3 times with DMF, 3 times with DCM, 5 times with DMF and 5 times with DCM. The Mtt group were then removed with a 1.8% TFA in DCM solution (9 times of 3 min each) [24].

2.5. Peptide cyclization

After removal of the Mtt group, the resin was washed 3 times with DCM, 3 times with DMF, 5 times with DCM and 5 times with DMF. On resin peptide cyclization was achieved by shaking for 48 h with 0.25 M DIEA in DMF [22].

2.6. Fatty acid acylation

After peptide cyclization, the resin was washed 3 times with DMF, 3 times with DCM and 5 times with DMF. Coupling of Lys, Asn and fatty acids were performed as in 2.2.

2.7. Peptide cleavage

The peptides were cleaved from the resin for 2 h using a freshly prepared cleavage cocktail (approximately 3 mL per 100 mg of resin) consisting of TFA/H_2O/TIS (95:2.5:2.5) (% *v/v*). Afterwards, the eluates were collected in centrifuge tubes and concentrated using a gentle stream of nitrogen. The peptides were precipitated and washed with cold Et_2O. After evaporation of the residual Et_2O, the peptides were dissolved in a H_2O/ACN mixture, and then left in a −80 °C freezer until frozen and lyophilized overnight.

2.8. Minimum inhibitory concentration and cytotoxicity assay

The antimicrobial activity were assessed using the broth micro dilution protocol adapted from Wiegand et al. [25] with minor modifications and cytotoxicity of the peptides were determined as previously described [26] with modifications (See supplementary materials S2).

2.9. Circular dichroism

See supplementary materials S2.

2.10. Small angle X-ray scattering

Unilamellar lipid vesicles were prepared using synthetic DMPC (1,2-dimyristoyl-sn-glycero-3-phosphocholine), DMPG (1,2-dimyristoyl-sn-glycero-3-phospho-(10-rac-glycerol)), and DMPE-PEG (1,2-dimyristoyl-sn-glycero-3-phosphoethanolamine-N-[methoxy(polyethylene glycol)-2000]) from Avanti Polar Lipids in the molar ratio 75:22.5:2.5. The lipids were first dissolved in a 1:3 methanol:chloroform solution. To make a lipid film the organic solvents were removed completely under vacuum using a Heidolph rotary evaporator with a Vacuubrand vacuum pump. The lipid film was rehydrated using a 50 mM Tris buffer, pH 7.4, at 35 °C. Then the dispersion was sonicated for 10 min to form smaller unilamellar vesicles, followed by extrusion of the lipid vesicles through a 100 nm pore diameter polycarbonate filter (>21 times) using an Avanti mini-extruder fitted with two 1 mL airtight syringes. Immediately before the SAXS data collection, a peptide solution with the adequate concentration for the target lipid:peptide ratio was mixed 1:1 with the lipid solution (5 mg/mL) using a micropipette.

SAXS experiments of the peptide-lipid mixes were performed at the automated BM29 bioSAXS beamline at the European Synchrotron Radiation Facility (ESRF) in Grenoble, France [27]. The data was obtained using an energy of 12.5 keV and a detector distance of 2.87 m, covering a Q range of about 0.0044 Å−1 to 0.51 Å−1. The data set was calibrated to an absolute intensity scale using water as a primary standard. 50 μL samples were run through a capillary using the flow mode of the automated sample changer [28]. SAXS data was collected in ten successive frames of 0.5 s each to monitor radiation damage and the data reduction was done using the standard tool at BM29 [29].

The SAXS results of the lipid vesicle-peptide mixtures were analyzed using the theoretical model described in detail by Nielsen et al. [16]. In short, the model provides a detailed description of the membrane by dividing into probability functions for each component (lipid sub-units/peptide) across the bilayer.

3. Results and discussion

A total of 19 *N*-locked cyclic analogues of indolicidin were successfully synthesized by Fmoc SPPS (**See Table 1**). Firstly, a lysine walk (1–13) was performed to investigate the influence of the increasing ring size on antimicrobial activity and cytotoxicity. Finally, 7 and 8 were chosen as structures to study the influence of lipidation (14–21). See supplementary materials S2-5 for peptide structures, MALDI-TOF-MS spectra and HPLC chromatograms.

3.1. The influence of the ring size on antimicrobial activity

In order to evaluate the optimal ring size for the antimicrobial activity of cyclic *N*-locked indolicidin analogues, we performed a lysine walk by systematically changing the position of the lysine residue from 1 to 13. Synthesis of 1 and 2 led to negligible yields, however we were able to see the correct mass (Not shown). We suspect this is due to the 1-residue and 2-residue macrocycle being an unfavorable reaction. Oddo et al. mention that the synthetic method is useful for an peptide macrocycle consisting of 3–13 residues [22]. We consequently decided not to pursue 1 and 2 any further. All compounds (3–13) showed similar in activity with MICs against *E. coli* ranging from 50 to >100 μg/mL, *P. aeruginosa* being >100 μg/mL, *S. aureus* from 12.5 to 50 μg/mL and *S. epidermidis* from 6.2 to 12.5 μg/mL, respectively. Interestingly, the loss of the cationic charge from the cyclization, probably causes the compounds (3–13) to lose antimicrobial activity against Gram-negative species (*E. coli* and *P. aeruginosa*) compared with indolicidin having MIC of 25 μg/mL against *E. coli* and MIC of 50 μg/mL against *P. aeruginosa*. Similarly, Staubitz et al. found that substituting Lys^5, Arg^{12} or Arg^{13} with alanine in linear indolicidin, resulted in great loss of activity against *E. coli* DH5α [17]. This is probably caused by the loss of one positive charge. Conversely, we have previously reported that substituting lys^1, lys^2, lys^5 or lys^7 with alanine in

Table 1
Sequence, minimum inhibitory concentration (μg/mL) and % viable HaCaT cells after 200 μg/mL peptide treatment.

No.	Sequence	EC [a]	PA [b]	SA [c]	SE [d]	%VC [e]
1[f]	c(K)–I-L-P-W-W-P-W-W-P-W-R-R-NH_2	–	–	–	–	–
2[f]	c(I–K)-L-P-W-W-P-W-W-P-W-R-R-NH_2	–	–	–	–	–
3	c(I-L-K)-P-W-W-P-W-W-P-W-R-R-NH_2	100	>100	50	6.3	71.5
4	c(I-L-P-K)-W-W-P-W-W-P-W-R-R-NH_2	50	>100	25	6.3	70.5
5	c(I-L-P-W-K)-W-P-W-W-P-W-R-R-NH_2	>100	>100	50	6.3	84.1
6	c(I-L-P-W-W-K)-P-W-W-P-W-R-R-NH_2	>100	>100	50	6.3	86.8
7	c(I-L-P-W-W-P-K)-W-W-P-W-R-R-NH_2	100	>100	12.5	6.3	84.3
8	c(I-L-P-W-W-P-W-K)-W-P-W-R-R-NH_2	100	>100	12.5	12.5	73.4
9	c(I-L-P-W-W-P-W-W-K)-P-W-R-R-NH_2	100	>100	25	6.3	92.2
10	c(I-L-P-W-W-P-W-W-P-K)-W-R-R-NH_2	>100	>100	25	12.5	100.3
11	c(I-L-P-W-W-P-W-W-P-W-K)-R-R-NH_2	100	>100	50	6.3	104.4
12	c(I-L-P-W-W-P-W-W-P-W-R-K)-R-NH_2	>100	>100	25	6.3	50.2
13	c(I-L-P-W-W-P-W-W-P-W-R-R-K)-NH_2	>100	>100	25	6.3	76.5
14[g]	c(I-L-P-W-W-P-K(C_6–N–K))–W–W–P–W-R-R-NH_2	100	>100	25	6.3	39.5
15[g]	c(I-L-P-W-W-P-K(C_8–N–K))–W–W–P–W-R-R-NH_2	>100	>100	25	6.3	49.6
16[g]	c(I-L-P-W-W-P-K(C_{10}–N–K))–W–W–P–W-R-R-NH_2	>100	>100	50	6.3	60.5
17[g]	c(I-L-P-W-W-P-K(C_{12}–N–K))–W–W–P–W-R-R-NH_2	>100	>100	>100	25	117.9
18[g]	c(I-L-P-W-W-P-W-K(C_6–N–K))–W–P–W-R-R-NH_2	>100	>100	25	6.3	46.5
19[g]	c(I-L-P-W-W-P-W-K(C_8–N–K))–W–P–W-R-R-NH_2	>100	>100	25	6.3	62.9
20[g]	c(I-L-P-W-W-P-W-K(C_{10}–N–K))–W–P–W-R-R-NH_2	>100	>100	50	6.3	75.2
21[g]	c(I-L-P-W-W-P-W-K(C_{12}–N–K))–W–P–W-R-R-NH_2	>100	>100	>100	12.5	127.9
Indolicidin	I-L-P-W-K-W-P-W-W-P-W-R-R-NH_2	25	50	25	3.1	11.3

Minimum inhibitory concentration were determined in triplicate by the broth microdilution method and reported in μg/mL. *E. coli* ATCC 25922 (EC) [a], *P. aeruginosa* H103 (PA) [b], *S. aureus* ATCC 29213 (SA) [c], *S. epidermidis* HJ56 (SE) [d]. % Viable HaCaT cells after 200 μg/mL peptide treatment (VC) [e]. We were not able to synthesize compound 1 and 2 in acceptable yields [f]. The K($C_{6\text{-}12}$-N-K) means that the lysine residue in the parenthesis is coupled to the secondary amine formed during cyclization (See Scheme 1) [g]. The $C_{6\text{-}12}$ respectively indicates one of the fatty acids, hexanoic acid (C_6), octanoic acid (C_8), decanoic acid (C_{10}) and dodecanoic acid (C_{12}). Residues in bold for 1–13 are changes relative to indolicidin, while for 14–17 are changes relative to 7 and for 18–21 are changes relative to 8.

a fully D-amino acid peptide D2D, resulted in retained activity both Gram-positive and Gram-negative species [30]. Therefore, the loss of antimicrobial activity against Gram-negatives is very sequence dependent. Antimicrobial activity against *S. aureus* compared with indolicidin either remained the same or improved by 2-fold with 7 and 8 having improved MICs of 12.5 μg/mL. Antimicrobial activity against *S. epidermidis* compared with indolicidin decreased by 4-fold for 8 and 10 and by 2-fold for the other compounds.

3.2. The influence of the ring size on cytotoxicity

All compounds (3–13) showed less cytotoxicity than indolicidin towards HaCaT cells after 200 μg/mL peptide treatment. The percent of viable HaCaT cells after treatment with 3–13 ranged from 50.2 to 104.4% compared to 11.3% viable HaCaT cells after indolicidin treatment. Especially 9, 10 and 11 showed significant improvement of 92.2, 100.3 and 104.4% viable HaCaT cells, respectively. 12 showed the lowest improvement with 50.2% viable HaCaT cells. The results demonstrate that *N*-locked cyclization can be a method to significantly reduce cytotoxicity. Similarly, Rozek et al. showed that a cyclic disulfide-bonded indolicidin analogue cycloCP-11, was less than 5% hemolytic against red blood cells at concentrations up to 256 μg/mL [19].

3.3. The influence of lipidation of 7 and 8 on antimicrobial activity

We decided to continue with 7 and 8 and investigate the effect of lipidation based on the antimicrobial activity and cytotoxicity of 3–13. Lipid tails attached directly to the rigid cyclic structure may give rise to analogues that possess only weak antimicrobial activity, Jensen et al. explains this by the lipid tail having limited flexibility when attached to the ring structure and therefor reducing its ability to insert efficiently into the bacterial membrane [31]. We therefore decided to insert the two residues lysine and asparagine between the macrocycle and the fatty acid as previously done by Oddo et al. [22]. Synthesis and purification of the peptides (14–21) were successful, however we observed poorer solubility in water stocks with increasing lipid tail length. The fatty acid acylation showed that 14–21 had similar antimicrobial activity of 100 to >100 μg/mL against the Gram-negative species *E. coli* and *P. aeruginosa* as compared to 3–13. Interestingly, MICs against *S. aureus* ranged from 25 to >100 μg/mL, worsening with increasing lipid tail length. An possible explanation could be that peptides with longer lipid tails in this case probably have induced an higher amount of aggregation, in agreement with the poor solubility observed. Malina et al. showed that lipidation can enchance or decrease the antibacterial activity of peptides, depending on the lipid tail length [32]. Antimicrobial activity against *S. epidermidis* remained more or less similar to 7 and 8.

3.4. The influence of lipidation on toxicity

All compounds (14–21) demonstated reduced cytotoxicity compared to indolicidin towards HaCaT cells after 200 μg/mL peptide exposure. However, increasing cytotoxicity was observed with shorter lipid tail length (See Table 1). The difference is easily demonstrated through the C_6 fatty acid compounds 14 and 18 showing cell viability of 39.5–46.5% after treatment, while the C_{12} fatty acid compounds 17 and 21 showed cell viability of 117.9–127.9% after treatment. The very high procentage viable HaCaT cells remaining after treatment with 17 and 21, may be an artifact from poor solubility rather than any cell proliferating effect. Conversely, Rounds et al. explain that the relationship between lipid chain length and cytotoxicity is difficult to determine as cytotoxicity is quantified in many different ways, but as a general observation state that a longer lipid tail length may lead to greater cytotoxicity [33].

3.5. Circular dichroism (CD)

The cyclic peptides without lipidation (3–13) were subjected to analysis by circular dichroism spectroscopy to assess any relevant variation of the peptide conformation in solution compared to indolicidin. The peptides all contain five Trp residues and these have a strong contribution to the observed CD signals in both the near and far UV regions (Fig. 1). Thus, the contribution of the backbone-based n-π* and π-π* transitions of the amide groups are not expected to make as significant an

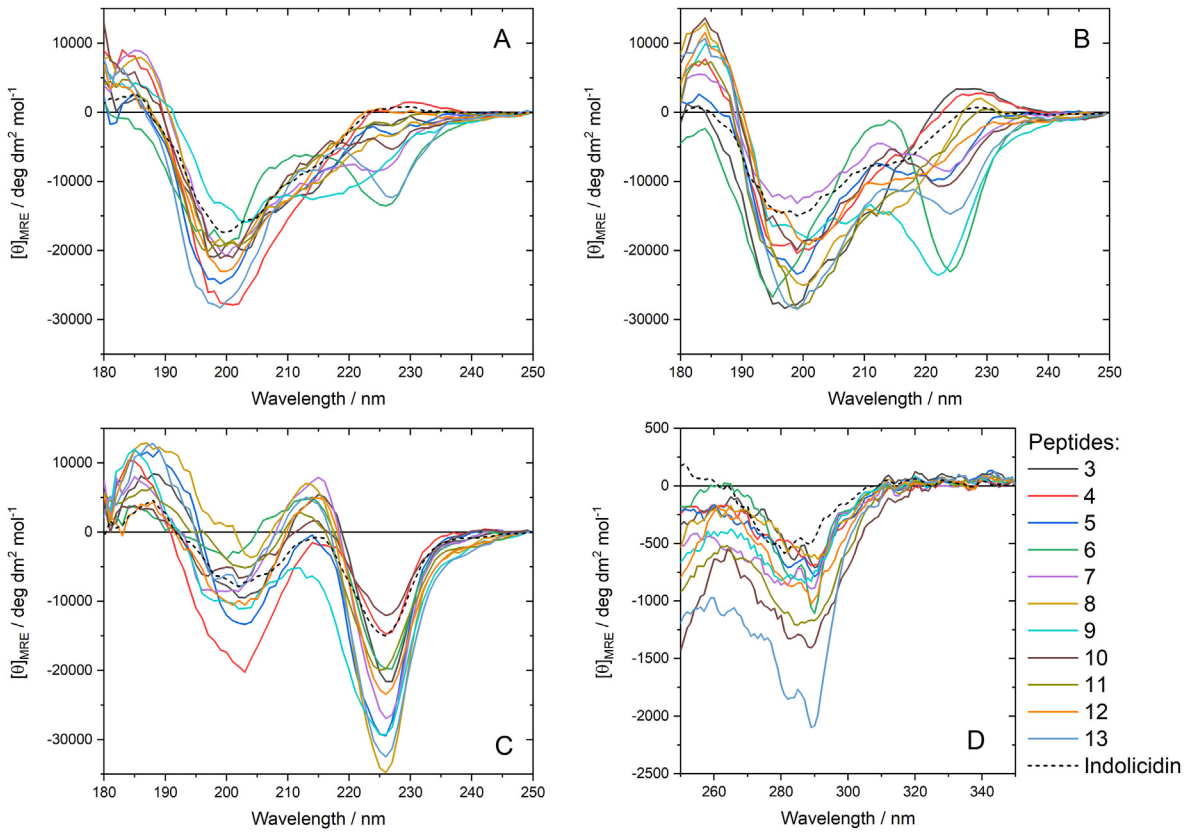

Fig. 1. UV Circular dichroism (CD) spectroscopy of 3–13 and indolicidin reported as mean residue ellipticity (MRE). Far-UV CD in Milli-Q water (A), 50% (v/v) 2,2,2-trifluoroethanol (B), 20 mM SDS (C) and near-UV CD in Milli-Q water (D).

impact to the spectra as for longer peptides with fewer aromatic groups. The Trp sidechain is known to have intense π-π* transitions in the far UV region. In the CD spectra these transitions may give rise to chiral signatures albeit with the complicating factor that individual Trp residues may experience a different environment yielding a positive or negative contribution in the same spectral region. An important aspect is the stacking of the aromatic Trp sidechains. The assignment of the far-UV CD of indolicidin and related peptides has been subject to a several studies including comparison between aqueous and membrane-mimicking solvents [14,34–36]. The presently studied series of peptides present an interesting case for analysis of Trp contributions to the CD spectra as they have an identical composition but explore different conformational space due to the incremental alteration of the ring-closure. It has been noted earlier [34,35] that the far-UV CD spectrum of indolicidin resembles that of a poly-L-proline helix which displays a large negative band at 202 nm and which may have a small positive band at 225 nm. However, the conformation of indolicidin does not assume this secondary structure, but is rather assumed to attain similar spectral features due to a combination of backbone turn conformation and the Trp contributions [34]. In Fig. 1A, the majority of peptides display similar spectra as indolicidin though typically with a stronger negative component at 200 nm. The peptides 6 and 13 both display a distinct negative band at around 225 nm, and peptides 7 and 9 also show negative components at slightly lower wavelengths. In Fig. 1B, the pure aqueous solution is exchanged for 50% 2,2,2-trifluoroethanol (TFE), a solvent known to induce α-helicity in a range of peptides [37], yet we observe no tendency for any of the studied peptides to assume any α-helix based on the CD data. Instead, an exaggeration of the negative band at 225 nm is observed for peptides 6 and 9 where the intensity is doubled. For peptide 6, it is clear that a positive component has appeared at 213 nm. This kind of positive-negative couplet is due to exciton splitting between proximal Trp chromophores [34]. In Fig. 1C, the solvent has been changed to a 20 mM SDS solution. We here see that the spectra for all peptides are transformed compared to pure water and display a clear and intense negative band at 225 nm with a positive component at ~215 nm and a weakened negative band at 202 nm compared to the data in panel A. In Fig. 1D, the near UV CD recorded in water is shown, and also here there are some marked differences between the peptides: Indolicidin itself displays the weakest signal and appears slightly blue-shifted compared to peptides 6 and 13. Indolicidin has local maxima at 288 nm, 281 nm, and 277 nm, whereas the two peptides have two main signals of vibrational fine structure at 289 nm and 282 nm with much greater intensity than the parent linear sequence. Several of the other peptides also display more intense CD signals in the near-UV than indolicidin, which likely represents the fact that the macrocycle formation does restrict the free rotation and solvent exposure of the Trp indole rings. In summary the far and near UV CD data point to a similar behavior for the ring-locked peptides, especially with regard to observations in solutions with SDS. It is noteworthy that the spectral features observed here in SDS solution resemble the spectral features seen in various types of other membrane-mimicking solvent mixtures. The effect of the surfactant appears to be a stabilization of conformers that can display exciton coupling between pairs of Trp side chains. Certain peptides, notably 6 and 13 display these spectral features in water and TFE and thus may have a structure similar to the consensus features seen in SDS. Thus, likely these peptides undergo a smaller conformational change upon changing from an aqueous to a surfactant solution. The previous conclusion that indolicidin displays no α-helicity can also be transferred here for the series of indolicidin-derived peptides.

3.6. Small angle X-ray scattering (SAXS)

The most active (based on MIC data) of the cyclic peptides without lipidation (7 and 8) were mixed with lipid vesicles in a small angle X-ray scattering (SAXS) experiment to study their membrane interaction. The

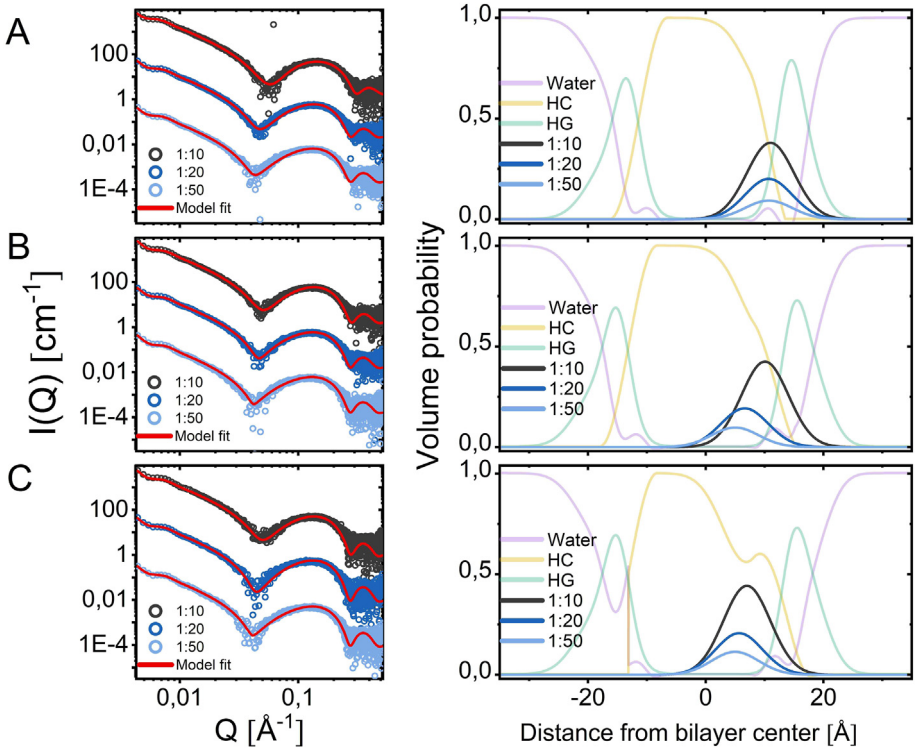

Fig. 2. Small angle X-ray scattering data of peptides mixed with lipid vesicles at different mixing ratio (peptide:lipid ratios indicated in legends) plotted together with best model fit, and the resulting volume probability plot calculated from fit parameters (HC: hydrocarbon chain groups, HG: head groups). Indolicidin (A), Peptide 7 (B), Peptide 8 (C).

same experiment was performed with indolicidin for comparison. The SAXS data plotted together with best fit is shown in Fig. 2. This approach allows us to extract both how these membrane active peptides affect the structure of the lipid vesicles (see supplementary material S8 for data on liposome reference without peptide), as well as the position of the peptide in the membrane as previously shown by Nielsen et al. [16].

Volume probability plots calculated from the fit parameters (supplementary material S9) reveal how all three peptides insert in the interface between the head and tail group of the outer leaflet of the membrane without detectably affecting the thickness of the membrane. This complies with previous reported SAXS data [16], and MD simulations results [38]. It has previously been hypothesized that indolicidin decreases the ordering of the lipids by changing the packing of the tails upon insertion in the outer leaflet which leads to a disruption of the permeability barrier imposed by the hydrocarbon core in the membrane [16,39]. It has further been reported that even though the thickness of the membrane is not affected significantly by insertion of indolicidin, the lipid dynamics including lipid inter-vesicular exchange and intra-vesicular lipid flip-flop is significantly accelerated upon peptide insertion [40]. Because both peptide 7 and 8 inserts into the same region of the membrane as indolicidin we suggest that the mechanism of action of these cyclic peptides are similar to that of indolicidin as described above. Especially, peptide 8 seem to insert slightly deeper into the lipid tail region (hydrocarbon chain groups), leading to potentially a slight larger effect on lipid packing and dynamical properties. However, the significance of this deeper penetration is yet to be fully clarified, especially considering the superior activity of indolicidin against every bacterial strain except *S. aureus* as seen from MIC data. Overall, the membrane interaction of these cyclic indolicidin analogues are determined to be similar to that of the natural peptide.

4. Conclusions

A library of 19 cyclic *N*-locked indolicidin analogues (3–21) were successfully synthesized in the present study. The peptides were cyclized by an on-resin strategy involving an intramolecular halide substitution of the *N*-terminus with an ε-amino lysine side chain. We found that a ring size consisting of 7 residues was most optimal for antibacterial activity against the Gram-positive bacteria, *S. aureus* and *S. epidermidis*. However, loss of activity was observed regardless of ring size against the Gram-negative bacteria, *E. coli* and *P. aeruginosa*. Nevertheless, cytotoxicity against HaCaT cells were greatly improved with cell viability ranging from 50.2 to 104.4%. Circular dichroism spectral data pointed to all peptides having a backbone turn conformation with significant spectral contributions from electronic transition of the indole groups of the Trp side chains. Peptides 6 and 13 especially showed a tendency to display Trp exciton coupling in aqueous solution – a trait assumed by indolicidin and the ring-locked analogues 3–13 in SDS conditions. SAXS together with theoretical modelling showed how the membrane interaction of peptide 7 and 8 is comparable to that of indolicidin, suggesting a similar mode of action. Acylation of cyclic *N*-locked indolicidin analogues with fatty acid of different lengths (14–21) showed no improvement of the antimicrobial activity. However, increasing cytotoxicity against HaCaT cells was seen with shorter lipid tail length. The most potent analogue identified was 7 with MIC of 12.5 μg/mL against *S. aureus*, 6.3 μg/mL against *S. epidermidis* and cell viability of 84.3%. In conclusion, this study demonstrates that *N*-locked cyclization of linear antimicrobial peptides can be utilized to develop novel leads with low cytotoxicity, although it may affect the antimicrobial activity.

Funding

This research was funded by Nordforsk: grant no. 82004.

Ethical approval

Not required.

Declaration of competing interest

The authors declare the following financial interests/personal relationships which may be considered as potential competing interests:

Håvard Jenssen reports financial support was provided by Nordforsk.

Acknowledgments

The authors would like to acknowledge David Gram Naym (Bispebjerg Hospital) for donating the HaCaT cell line. Furthermore, we thank Kirsten Olesen, Yasemin Karatas and Birgitte Simonsen for excellent technical assistance. The authors are grateful to the ESRF for providing Beamtime and for the assistance by Dr. Petra Pernot at ESRF with performing remote BM29 SAXS experiment. We also, thank Victoria Ariel Bjørnestad and Kari Kristine Almåsvold Borgos for preparation of samples for the SAXS experiment.

Appendix A. Supplementary data

Supplementary data to this article can be found online at https://doi.org/10.1016/j.ejmcr.2022.100080.

References

[1] R. Gaynes, The discovery of penicillin—new insights after more than 75 Years of clinical use, Emerg. Infect. Dis. 23 (2017) 849–853.
[2] J. Carlet, V. Jarlier, S. Harbarth, A. Voss, H. Goossens, D. Pittet, Ready for a world without antibiotics? The pensières antibiotic resistance call to action, Antimicrob. Resist. Infect. Control 1 (2012) 11.
[3] M.S. Mulani, E.E. Kamble, S.N. Kumkar, M.S. Tawre, K.R. Pardesi, Emerging strategies to combat ESKAPE pathogens in the era of antimicrobial resistance: a review, Front. Microbiol. 10 (2019), https://doi.org/10.3389/fmicb.2019.00539.
[4] N. Mookherjee, M.A. Anderson, H.P. Haagsman, D.J. Davidson, Antimicrobial host defence peptides: functions and clinical potential, Nat. Rev. Drug Discov. 19 (2020) 311–332.
[5] H. Jenssen, P. Hamill, R.E.W. Hancock, Peptide antimicrobial agents, Clin. Microbiol. Rev. 19 (2006) 491–511.
[6] N. Molchanova, P.R. Hansen, H. Franzyk, Advances in development of antimicrobial peptidomimetics as potential drugs, Molecules 22 (2017) 1430.
[7] H. Etayash, D. Pletzer, P. Kumar, S.K. Straus, R.E.W. Hancock, Cyclic derivative of host-defense peptide IDR-1018 improves proteolytic stability, suppresses inflammation, and enhances in vivo activity, J. Med. Chem. 63 (2020) 9228–9236.
[8] A. Lone, A. Arnous, P.R. Hansen, B. Mojsoska, H. Jenssen, Synthesis of peptoids containing multiple nhtrp and ntrp residues: a comparative study of resin, cleavage conditions and submonomer protection, Front. Chem. 8 (2020), 370-370.
[9] R.N. Zuckermann, J.M. Kerr, S.B.H. Kent, W.H. Moos, Efficient method for the preparation of peptoids [oligo(N-substituted glycines)] by submonomer solid-phase synthesis, J. Am. Chem. Soc. 114 (1992) 10646–10647.
[10] M.E. Selsted, M.J. Novotny, W.L. Morris, Y.Q. Tang, W. Smith, J.S. Cullor, Indolicidin, a novel bactericidal tridecapeptide amide from neutrophils, J. Biol. Chem. 267 (1992) 4292–4295.
[11] T.J. Falla, D.N. Karunaratne, R.E.W. Hancock, Mode of action of the antimicrobial peptide indolicidin, J. Biol. Chem. 271 (1996) 19298–19303.
[12] H.J. Schluesener, S. Radermacher, A. Melms, S. Jung, Leukocytic antimicrobial peptides kill autoimmune T-cells, J. Neuroimmunol. 47 (1993) 199–202.
[13] A. Rozek, C.L. Friedrich, R.E.W. Hancock, Structure of the bovine antimicrobial peptide indolicidin bound to dodecylphosphocholine and sodium dodecyl sulfate micelles, Biochem. 39 (2000) 15765–15774.
[14] C.L. Friedrich, A. Rozek, A. Patrzykat, R.E.W. Hancock, Structure and mechanism of action of an indolicidin peptide derivative with improved activity against gram-positive bacteria, J. Biol. Chem. 276 (2001) 24015–24022.
[15] J.E. Nielsen, T.K. Lind, A. Lone, Y. Gerelli, P.R. Hansen, H. Jenssen, M. Cárdenas, R. Lund, A biophysical study of the interactions between the antimicrobial peptide indolicidin and lipid model systems, Biochim. Biophys. Acta Biomembr. 1861 (2019) 1355–1364.
[16] J.E. Nielsen, V.A. Bjørnestad, R. Lund, Resolving the structural interactions between antimicrobial peptides and lipid membranes using small-angle scattering methods: the case of indolicidin, Soft Matter 14 (2018) 8750–8763.
[17] P. Staubitz, A. Peschel, W.F. Nieuwenhuizen, M. Otto, F. Götz, G. Jung, R.W. Jack, Structure–function relationships in the tryptophan-rich, antimicrobial peptide indolicidin, J. Pept. Sci. 7 (2001) 552–564.
[18] T.S. Ryge, X. Doisy, D. Ifrah, J.E. Olsen, P.R. Hansen, New indolicidin analogues with potent antibacterial activity, J. Pept. Res. 64 (2004) 171–185.
[19] A. Rozek, J.P.S. Power, C.L. Friedrich, R.E.W. Hancock, Structure-based design of an indolicidin peptide analogue with increased protease stability, Biochem. 42 (2003) 14130–14138.
[20] T. Velkov, P.E. Thompson, R.L. Nation, J. Li, Structure−Activity relationships of polymyxin antibiotics, J. Med. Chem. 53 (2010) 1898–1916.
[21] N.N. Mishra, S.J. Yang, L. Chen, C. Muller, A. Saleh-Mghir, S. Kuhn, A. Peschel, M.R. Yeaman, C.C. Nast, B.N. Kreiswirth, A.C. Crémieux, A.S. Bayer, Emergence of daptomycin resistance in daptomycin-naïve rabbits with methicillin-resistant Staphylococcus aureus prosthetic joint infection is associated with resistance to host defense cationic peptides and mprF polymorphisms, PLoS One 8 (2013), e71151.
[22] A. Oddo, L. Münzker, P.R. Hansen, Peptide macrocycles featuring a backbone secondary amine: a convenient strategy for the synthesis of lipidated cyclic and bicyclic peptides on solid support, Org. Lett. 17 (2015) 2502–2505.
[23] P.R. Hansen, A. Oddo, Fmoc solid-phase peptide synthesis, in: G. Houen (Ed.), Peptide Antibodies: Methods and Protocols, Springer New York, New York, NY, 2015, pp. 33–50.
[24] D. Li, D.L. Elbert, The kinetics of the removal of the N-methyltrityl (Mtt) group during the synthesis of branched peptides, J. Pept. Res. 60 (2002) 300–303.
[25] I. Wiegand, K. Hilpert, R.E.W. Hancock, Agar and broth dilution methods to determine the minimal inhibitory concentration (MIC) of antimicrobial substances, Nat. Protoc. 3 (2008) 163–175.
[26] M.V. Mouritzen, , et al.S. Abourayale, R. Ejaz, C.B. Ardon, E. Carvalho, L.T. Dalgaard, M. Roursgaard, H. Jenssen, Neurotensin, substance P, and insulin enhance cell migration, J. Pept. Sci. 24 (7) (2018), e3093.
[27] P. Pernot, A. Round, R. Barrett, A.D.M. Antolinos, A. Gobbo, E. Gordon, J. Huet, J. Kieffer, M. Lentini, M. Mattenet, C. Morawe, C. Mueller-Dieckmann, S. Ohlsson, W. Schmid, J. Surr, P. Theveneau, L. Zerrad, S. McSweeney, Upgraded ESRF BM29 beamline for SAXS on macromolecules in solution, J. Synchrotron Radiat. 20 (2013) 660–664.
[28] A. Round, F. Felisaz, L. Fodinger, A. Gobbo, J. Huet, C. Villard, C.E. Blanchet, P. Pernot, S. McSweeney, M. Roessle, D.I. Svergun, F. Cipriani, BioSAXS Sample Changer: a robotic sample changer for rapid and reliable high-throughput X-ray solution scattering experiments, Acta Crystallogr. D17 (2015) 67–75.
[29] A.D.M. Antolinos, P. Pernot, M.E. Brennich, J. Kieffer, M.W. Bowler, S. Delageniere, S. Ohlsson, S.M. Monaco, A. Ashton, D. Franke, D. Svergun, S. McSweeney, E. Gordon, A. Round, ISPyB for BioSAXS, the gateway to user autonomy in solution scattering experiments, Acta Crystallogr. D71 (2015) 76–85.
[30] A. Lone, T.T. Thomsen, J.E. Nielsen, P.W. Thulstrup, R.N. Klitgaard, A. Løbner-Olesen, R. Lund, H. Jenssen, P.R. Hansen, Structure-activity study of an all-d antimicrobial octapeptide D2D, Molecules 24 (2019) 4571.
[31] S.K. Jensen, T.T. Thomsen, A. Oddo, H. Franzyk, A. Løbner-Olesen, P.R. Hansen, Novel cyclic lipopeptide antibiotics: effects of acyl chain length and position, Int. J. Mol. Sci. 21 (2020) 5829.
[32] A. Malina, Y. Shai, Conjugation of fatty acids with different lengths modulates the antibacterial and antifungal activity of a cationic biologically inactive peptide, Biochem. J. 390 (2005) 695–702.
[33] T. Rounds, S.K. Straus, Lipidation of antimicrobial peptides as a design strategy for future alternatives to antibiotics, Int. J. Mol. Sci. 21 (2020) 9692.
[34] A.S. Ladokhin, M.E. Selsted, S.H. White, CD spectra of indolicidin antimicrobial peptides suggest turns, not polyproline helix, Biochem. 38 (1999) 12313–12319.
[35] V.V. Andrushchenko, H.J. Vogel, E.J. Prenner, Solvent-dependent structure of two tryptophan-rich antimicrobial peptides and their analogs studied by FTIR and CD spectroscopy, Biochim. Biophys. Acta 1758 (2006) 1596–1608.
[36] A.L.C.F. Souto, E.F. Poletti, C.R. Nakaie, S. Schreier, in: F. Galembeck (Ed.), Fluorescence and Circular Dichroism Study of the Interaction between Indolicidin, a Tryptophan-Rich Antimicrobial Peptide, and Model Membranes, Surface and Colloid Science, 2004, pp. 203–206.
[37] M. Buck, Trifluoroethanol and colleagues: cosolvents come of age. Recent studies with peptides and proteins, Q. Rev. Biophys. 31 (1998) 297–355.
[38] J.C.Y. Hsu, C.M. Yip, Molecular dynamics simulations of indolicidin association with model lipid bilayers, Biophys. J. 92 (2007) L100–L102.
[39] W.C. Wimley, Describing the mechanism of antimicrobial peptide action with the interfacial activity model, ACS Chem. Biol. 5 (2010) 905–917.
[40] J.E. Nielsen, V.A. Bjørnestad, V. Pipichi, H. Jenssen, R. Lund, Beyond structural models for the mode of action: how natural antimicrobial peptides affect lipid transport, J. Colloid Interface Sci. 582 (2021) 793–802.